Colloid Polym Sci 278:764–770 (2000)

ORIGINAL CONTRIBUTION

B. Jean
L.-T. Lee
B. Cabane

Interactions of sodium dodecyl sulfate with acrylamide – *N*-isopropylacrylamide) statistical copolymer

Received: 11 November 1999
Accepted: 15 December 1999

B. Jean · L.-T. Lee (✉)
Laboratoire Léon Brillouin, CEA-Saclay
91191 Gif-sur-Yvette Cedex, France

B. Cabane
PMMH, ESPCI, 10 rue Vauquelin
75231 Paris Cedex 05, France

Abstract Poly(*N*-isopropylacrylamide) (PNIPAM) precipitates out of water around 32 °C. This critical temperature is raised when hydrophilic acrylamide sequences are present on the polymer chain. We have used neutron scattering to study the structural properties of a statistical copolymer containing acrylamide and *N*-isopropylacrylamide segments at different temperatures and its interactions with an anionic surfactant, sodium dodecyl sulfate (SDS). At low temperatures, the copolymer behaves as a swollen polymer coil. With an increase in temperature, intermolecular attractions are observed, and close to the critical temperature of the copolymer, microphase separation is observed. Here, the structure consists of dense nodules of hydrophobic sequences stabilized by hydrophilic sequences. In the presence of a small amount of SDS, additional colloidal stability is observed: the nodule size is decreased. At high SDS concentration, the copolymer is completely solubilized at all temperatures studied and the structure of the polymer–surfactant complex resembles the "necklace" structure obtained for the homopolymer PNIPAM–SDS system.

Key words Statistical copolymer · Neutron scattering · Polymer-surfactant interactions

Introduction

Poly(*N*-isopropylacrylamide) (PNIPAM) is a nonionic water-soluble polymer that exhibits inverse solubility behavior: it precipitates out of water when heated above the lower critical solution temperature (LCST) of about 32 °C. The isopropyl side group carried by each monomer of PNIPAM confers a small degree of hydrophobic character and is responsible for the surface activity and interaction with surfactants such as sodium dodecyl sulfate (SDS). There has been much work done on the solution properties of the PNIPAM–SDS system [1] as well as on the structures of the polymer–surfactant complex that is formed [2].

In this study, we are interested in the behavior of a copolymer containing both hydrophobic and hydrophilic segments. The polymer that we have chosen is a statistical copolymer, AM40-*co*-NIPAM60, containing 40% acrylamide (AM) and 60% *N*-isopropylacrylamide (NIPAM) units. Polyacrylamide (PAM) is a hydrophilic polymer exhibiting an upper critical solution temperature [3] and is soluble in water at all positive temperatures. PAM does not interact with SDS [4].

AM40-*co*-NIPAM60 therefore contains both hydrophobic and hydrophilic sequences. In addition, the degree of hydrophobicity of the NIPAM units can be varied by changing the temperature, while the AM units remain completely hydrophilic. Thus, while PNIPAM homopolymer has an LCST of around 32 °C, AM40-*co*-NIPAM60 has an LCST of around 75 °C [5]. In this study, we are interested in the behavior of the copolymer when the temperature is raised above that of the LCST of the PNIPAM homopolymer: how will the two types of monomers associate or segregate to accommodate the change in solvent quality? Furthermore, knowing that SDS interacts only with the PNIPAM sequences of the copolymer, what are the effects of the addition of surfactant molecules to AM40-*co*-NIPAM60 solutions? The interaction of this copolymer with SDS has been studied by fluorescence and viscosity measurements [5]. Here, we focus on the structures of aqueous solutions of AM40-*co*-NIPAM60 and SDS as a function of temperature and concentration using small-angle neutron scattering, a technique which permits us to study separately the structure of each component in a mixed polymer–surfactant complex.

Materials and methods

Materials

AM40-*co*-NIPAM60 copolymer was a generous gift from Dr. G. Staikos (University of Patras, Greece). It was prepared using a redox polymerization method; its molecular weight determined by viscometry is 2.5×10^5 and the LCST deduced from visual observation is about 75 °C [5]. Deuterated SDS was purchased from Isotec, France, and was used as received. The solution mixtures were prepared at fixed polymer concentration, c_p (0.01 or 0.03 g/ml) and increasing surfactant concentration, thus varying the surfactant/polymer ratio, S/P. In this study, $0 \leq S/P \leq 1$.

Neutron scattering

The scattering experiments were performed on the D11 and D22 instruments at ILL, Grenoble, and on the PAXE instrument at LLB, Saclay. Isotopic substitution of H by D allows us to vary the contrast of the components and thus study scattering from polymer and from surfactant separately. In the scattering from the polymer, protonated copolymer, deuterated SDS and pure D_2O are used. In this contrast scheme, deuterated SDS is almost contrast-matched to pure D_2O and the scattering signal is predominantly due to the copolymer. In the scattering from SDS, protonated copolymer, deuterated SDS and a 20% D_2O–80% H_2O volume mixture are used. The protonated copolymer is contrast-matched to this solvent mixture and scattering is mostly from SDS. In each case, the scattered intensity was recorded at 20, 40, 60 and about 70 °C.

Results

Scattering from copolymer alone

The scattering curves of the copolymer alone at different temperatures are shown in Fig. 1. At 20 °C, the scattering curve is typical of that obtained for swollen polymer coils in a good solvent. A good approximation to the complete shape of the scattering function is provided by the Fisher–Burford formula [6]:

$$\frac{I(q)}{I(0)} = \left[1 + \frac{(q\xi)^2}{(3d_f/2)}\right]^{(-d_f/2)} , \qquad (1)$$

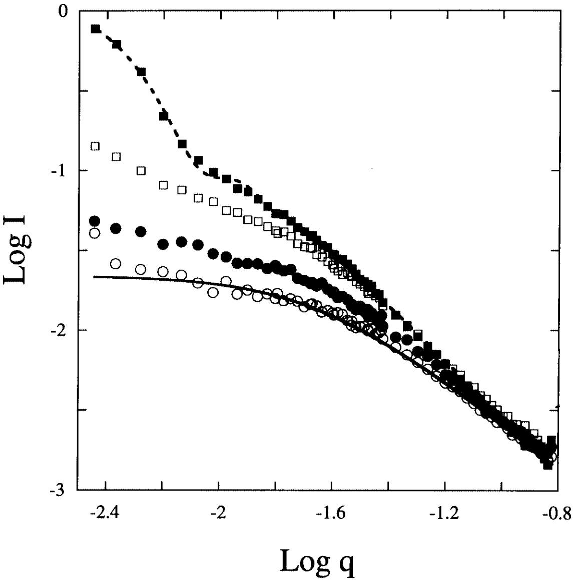

Fig. 1 Scattering from a copolymer containing 40% acrylamide (*AM*) and 60% N-isopropylacrylamide (*NIPAM*) (AM40-*co*-NIPAM60) at c_p = 0.03 g/ml and different temperatures: 20 °C (*open circles*); 40 °C (*filled circles*); 60 °C (*open squares*); 70 °C (*filled squares*). The *continuous line* is a fit using the Fisher–Burford approximation (Eq. 1). The *dashed line* is a fit using the two-population model (Eq. 2)

where ξ is a correlation length characterizing the largest heterogeneity and d_f is an exponent characterizing the power-law decay at higher q and which is analogous to a fractal dimension. At 20 °C, the fit using Eq. (1) gives a $q^{-1.49}$ decay instead of the $q^{-1.67}$ decay expected for the configurational statistics of swollen polymer coils in a good solvent. This difference is not significant considering the reduced q range where the power law is observed. The correlation lengths obtained are 60 and 130 Å at c_p = 3 and 1%, respectively.

For $T \geq 40$ °C, the scattered intensity increases when q tends to zero, indicating the presence of larger objects (aggregation). At 40 °C, which is above the LCST of pure PNIPAM, the increase in $I(q \to 0)$ is still modest. At the same temperature, an aqueous solution of PNIPAM homopolymer phase-separates, and the scattering curve exhibits a q^{-4} decay, which is a signature of a two-phase sample [2].

At $T \sim 70$ °C, the scattering intensity at $q \to 0$ is 33 times higher than at 20 °C, indicating the presence of large finite aggregates at this temperature; however, the high-q region of the scattering curve remains nearly unchanged, suggesting the presence of solubilized polymer chains even at this elevated temperature. The dashed line is a fit using a linear combination of the scattered intensity by large objects (spheres of radius R) and the scattered intensity by macromolecules in a good solvent (Fisher–Burford approximation used at 20 °C):

$$I(q) = A\left(1 + \frac{(q\xi)^2}{(3d_f/2)}\right)^{(-d_f/2)} + B\left(\frac{3[\sin(qR) - qR\cos(qR)]}{(qR)^3}\right)^2 . \quad (2)$$

The good agreement between this simple two-population model and the experimental data suggests that at this high temperature close to the LCST, the system consists of dense nodules coexisting with solubilized chains. The size of the large objects obtained is 490 Å (Table 1).

Scattering from copolymer in the presence of surfactant

S/P = 0.1

The scattering curves of the copolymer with S/P = 0.1 at different temperatures are shown in Fig. 2. Note that at 60 °C, the scattering at low q is essentially flat, whereas a continuous increase is observed in the absence of SDS (Fig. 1). Moreover, when the temperature is raised from 20 to 60 °C the intensity at $q = 0$ is increased by a factor of 2 for S/P = 0.1 compared to a factor of 6 for S/P = 0. These two observations suggest that at 60 °C the presence of SDS limits the aggregation of the macromolecules. A Zimm plot of the data gives lower ξ values for S/P = 0.1 than for S/P = 0 (Table 2). The solid line through the scattering curve at $T \sim 70$ °C is a fit of the data using the two-population model (Eq. 2). The good agreement between the model and the experimental data again reveals the bipopulated behavior (see Table 1 for values of the fitted parameters).

S/P ≥ 0.3

In the presence of larger amounts of SDS, the copolymer is completely solubilized and the scattering curves show a depression at low q followed by a peak (Fig. 3). The depression indicates that the macromolecules repel each other. This repulsion peak has been reported in other systems [2, 7, 8] and has been attributed to electrostatic interactions of surfactant micelles bound to the polymer chains. The depression becomes deeper as the surfactant concentration increases and is observed even at S/P = 1. This suggests that there is no significant amount of free (unbound) micelles, the presence of which would have screened the intermolecular interactions. The peak corresponds to a real space distance, ξ, between macromolecules loaded with charged surfactant micelles. When S/P increases, the peak position moves towards higher q values and $I(q_{\max})$ and $I(q_{\to 0})$ decrease. This process may be similar to the charging up of a weakly charged polyelectrolyte in the semidilute regime [9, 10].

The temperature dependence of these samples containing large amounts of surfactant is quite different from those containing little or no surfactant: there is only a very slight influence of temperature at S/P = 0.3 and 0.5 and none at all at higher S/P values (Fig. 4).

Table 1 Fitted results using the two-population model (Eq. 2) for solutions of a copolymer containing 40% acrylamide (*AM*) and 60% *N*-isopropylacrylamide (*NIPAM*) (AM40-*co*-NIPAM60) at $c_p = 0.03$ g/ml and $T \sim 70$ °C with a surfactant/polymer ratio, S/P = 0 and S/P = 0.1

Parameters	S/P = 0	S/P = 0.1
A	0.146	0.06
ξ (Å)	146	43
d_f	1.8	3.2
B	1.24	0.2
R (Å)	490	200

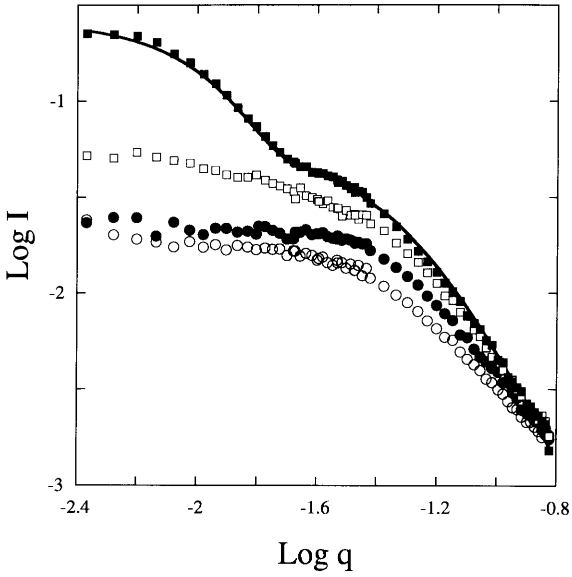

Fig. 2 Scattering from AM40-*co*-NIPAM60 at $c_p = 0.03$ g/ml and a surfactant/polymer ratio, S/P = 0.1 at different temperatures: 20 °C (*open circles*); 40 °C (*filled circles*); 60 °C (*open squares*); ~70 °C (*filled squares*). The *continuous line* is a fit using the two-population model (Eq. 2)

Table 2 Blob sizes of AM40-*co*-NIPAM60 calculated from the slopes and intercepts of $c_p/I(q)$ versus q^2 plots ($c_p = 0.03$ g/ml)

T (°C)	ξ_b (Å) S/P = 0	ξ_b (Å) S/P = 0.1
20	85	61
40	100	63
60	145	100

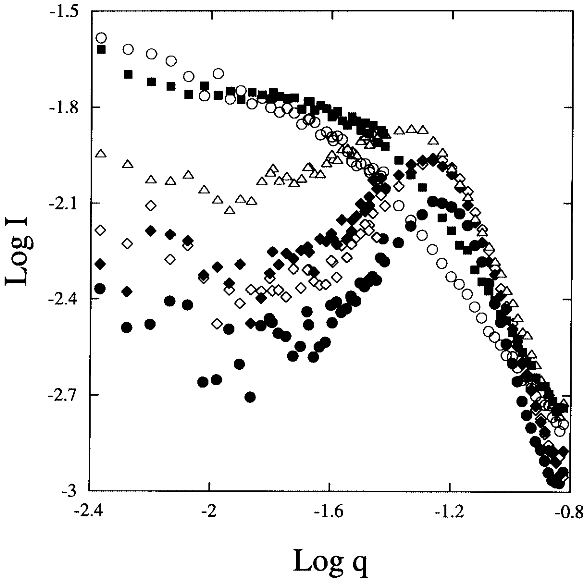

Fig. 3 Scattering from AM40-*co*-NIPAM60 at $c_p = 0.03$ g/ml and different S/P at 20 °C: S/P = 0 (*open circles*); S/P = 0.1 (*filled squares*); S/P = 0.3 (*open triangles*); S/P = 0.5 (*filled diamonds*); S/P = 0.7 (*open diamonds*); S/P = 1 (*filled circles*)

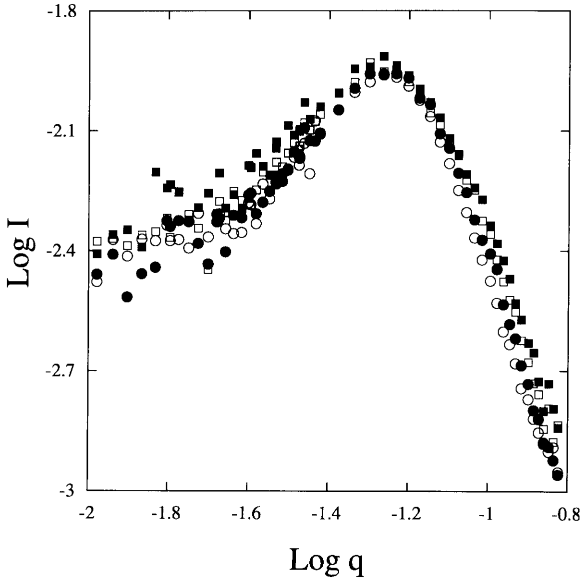

Fig. 4 Scattering from AM40-*co*-NIPAM60 at $c_p = 0.03$ g/ml and S/P = 0.7 at different temperatures: 20 °C (*open circles*); 40 °C (*filled circles*); 60 °C (*open squares*); ~70 °C (*filled squares*)

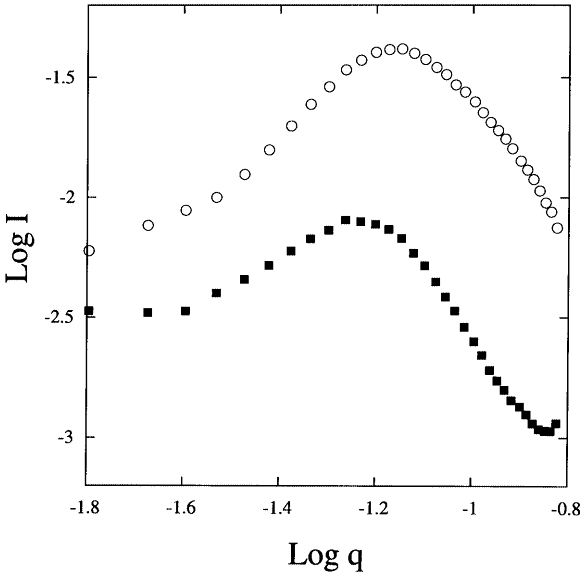

Fig. 5 Scattering from samples at $c_p = c_s = 0.03$ g/ml and 20 °C: surfactant scattering (*open circles*); copolymer scattering (*filled squares*)

Scattering from surfactant

At high surfactant concentration, the surfactant scattering curve also shows a repulsion peak. This can be seen in Fig. 5 for $c_p = 0.03$ g/ml and S/P = 1. The location of this peak corresponds to a characteristic distance, ξ_m. This is an intermicellar distance which is a little smaller than, but of the same order as, the interchain distance observed in the polymer scattering (also shown in the same figure). Both ξ and ξ_m decrease with S/P but are unaffected by temperature. The scattered intensity of the surfactant increases with concentration and decreases with temperature (Fig. 6; see also Table 3).

When the polymer concentration is diluted to 0.01 g/ml, the surfactant scattering curve shows two peaks: a first peak, already described, corresponding to ξ_m (which is equal to ξ at this polymer concentration) and a second peak which is situated at a higher q range, corresponding to a real space distance d = 90 Å at 20 °C (Fig. 7). The value of d is the same as that found for SDS micelles bound to PNIPAM homopolymer at the same temperature [2]. It remains independent of the surfactant concentration in the range $0.5 \leq \mathrm{S/P} \leq 1$ and is interpreted as the distance between consecutive micelles bound to the same macromolecule [2, 7, 8]. This shorter distance can be better observed at lower chain concentration since its corresponding peak is located further away from the peak of the interchain distance (160 Å at $c_p = 0.01$ g/ml and 109 Å at $c_p = 0.03$ g/ml, S/P = 1). The separation of these two intermicellar distances may also explain why at lower polymer concentration ξ_m is equal to ξ, while at higher polymer concentration ξ_m is slightly smaller than ξ due to an averaging effect of ξ_m.

In Fig. 7, note also that the polymer scattering curve shows an oscillation at high q. This oscillation corresponds to a real space distance h = 34 Å. This feature, which appears only in the presence of SDS, has also been observed for the PNIPAM homopolymer system

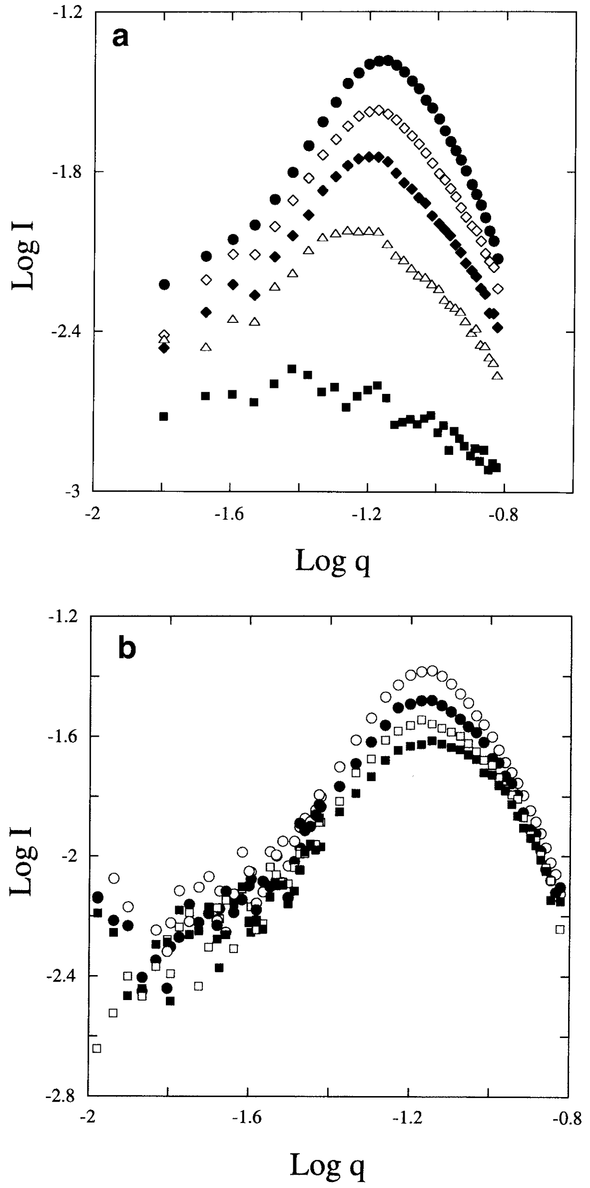

Fig. 6 a Scattering from sodium dodecyl sulfate (*SDS*) at $c_p = c_s = 0.03$ g/ml and different S/P at 20 °C: S/P = 0.1 (*filled squares*); S/P = 0.3 (*open triangles*); S/P = 0.5 (*filled diamonds*); S/P = 0.7 (*open diamonds*); S/P = 1.0 (*filled circles*). **b** Scattering from SDS at $c_p = c_s = 0.03$ g/ml and S/P = 1.0 at different temperatures: 20 °C (*open circles*); 40 °C (*filled circles*); 60 °C (*open squares*); ~70 °C (*filled squares*)

and is interpreted as a feature due to polymer segments associated with the micelles.

Discussion

S/P = 0

Table 3 Interchain (ξ) and intermicellar (ξ_m) distances determined from the peak positions in the scattering curves from copolymer and from surfactant at $c_p = 0.03$ g/ml and T = 20 °C

S/P	ξ (Å)	ξ_m (Å)
0.3	134	110
0.5	121	101
0.7	116	96
1	109	92

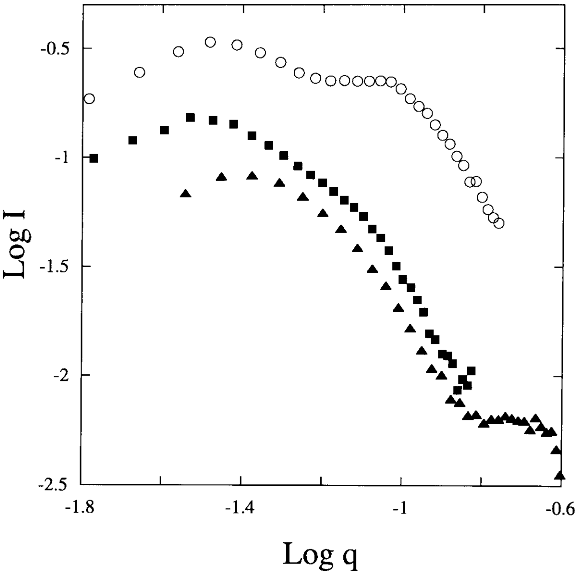

Fig. 7 Scattering from samples at c_s = 0.01 g/ml at 20 °C: scattering from surfactant at S/P = 1.0 (*open circles*); scattering from copolymer at S/P = 1.0 (c_p = 0.01 g/ml) (*filled squares*); scattering from copolymer at S/P = 0.5 (c_p = 0.02 g/ml) (*filled triangles*)

The evolution of the AM40-*co*-NIPAM60 copolymer structure in aqueous solution has been studied between 20 and around 70 °C. At 20 °C, all the monomers constituting the copolymer are in a good solvent and the copolymer behaves as a solubilized coil. Little effect is observed when the temperature is raised from 20 to 40 °C although this temperature is above the LCST of pure PNIPAM. This suggest that the PNIPAM sequences in the copolymer are relatively short. At 60 °C, the increase in $I(q_{\to 0})$ shows an increasing attraction between macromolecules. Finally, at $T \sim 70$ °C, close to the LCST of the copolymer, a microphase rather than a macrophase separation is observed. The scattering curve of AM40-*co*-NIPAM60 at this temperature is a superposition of scattering from large objects modeled by dense spheres of radius $R = 490$ Å and the scattering from solubilized chains. The dense particles are presumably mainly constituted of collapsed NIPAM monomers and the solubilized chains of AM monomers. This may reflect two possible situations: either there is a coexistence of the two separate types of objects in the solution or there is only one type of object consisting of hairy particles with a dense inner core. In the first case, nothing can prevent aggregation of the dense particles from occurring and this situation would lead to a macroscopic phase separation. In the second case, hairy soluble sequences around the dense nodules would prevent their aggregation by steric stabilization. These soluble sequences would be AM-rich sequences which are unaffected by temperature. The size of these colloidal objects depends on the sequences since long enough AM-rich parts are required for steric stabilization. This second situation is compatible with a statistical copolymer. A copolymer with alternating monomers is not compatible with a bipopulated system because long enough NIPAM and AM are necessary to create such a structure.

S/P = 0.1

As shown by the shape of the curves at low q, when the temperature is raised from 20 to 60 °C, the attraction between macromolecules is reduced in the presence of a small amount of SDS. Adsorption of SDS molecules introduces weak electrostatic repulsion effects, which lower the aggregation tendency when the temperature is increased. Thus, for $T \leq 60$ °C, surfactant molecules hinder aggregation.

At $T \sim 70$ °C, the samples appear to have two associated structures, as observed in the absence of surfactant. Here as well, the objects may be interpreted as a collection of hairy colloidal particles; however, in the presence of a small amount of SDS, the nodule that forms the dense core of the particle is 2.5 times smaller (R = 200 Å) than in the absence of SDS (R = 490 Å). This new size is the result of a balance between hydration forces of AM-rich sequences, hydrophobic effects that cause NIPAM monomers to segregate and electrostatic forces introduced by adsorption of SDS.

S/P ≥ 0.3

In this range of S/P ratio, the AM40-*co*-NIPAM60 copolymer is completely dissolved by SDS at all the temperatures studied. All the features given by the scattering curves from the copolymer and from the surfactant show that the surfactant micelles and the copolymer are associated in the same manner as in other neutral polymer and anionic surfactants such as polyethylene oxide (PEO) + SDS [7, 8] and PNIPAM + SDS [2]; therefore, the system can be described, at all temperatures, as a solution of "necklaces", each necklace being constituted of one macromolecule and several bound micelles.

In the range 0.5 ≤ S/P ≤ 1, the surfactant scattering curves for c_p = 0.01 g/ml at 20 °C show that the distance between consecutive micelles along a necklace remains unchanged at 90 Å. This value is similar to the d values found for PEO + SDS [7, 8] and PNIPAM + SDS [2] at the same temperature. At $T \sim 70$ °C, d is found to be lower, around 70 Å. This value is close to that obtained for SDS + PNIPAM homopolymer at 40 °C (63 Å) [2]. This distance is governed by a balance between attractions originating from the adsorption strength of PNIPAM on the micelles, which increases with temperature, and electrostatic repulsion between charged micelles.

Variation of the peak position at intermediate q

The scattering curves show variations of the peak position at intermediate q (corresponding to ξ) with chain concentration. Such a variation is expected for charged rodlike objects. For weakly charged polyelectrolytes in semidilute condition, theory predicts [11, 12] that the peak position varies as $q_{\max} \sim f^{1/3}c^{1/2}$, where f is the charge density and c the chain concentration. This relation is valid for values of f lower than the limit of the Manning condensation, $f_0 = a/L_B$. Taking L_B = 7.16 Å at 25 °C and a = 2.5 Å for PNIPAM [13], $f_0 = 0.35$. In the present study, if we consider that for S/P ≤ 1.0 all the SDS molecules are adsorbed on the polymer chain, the charge density is given by $f = (M_{\text{monomer}}/M_{\text{SDS}}) \times (\text{S/P}) = 0.307 \times (\text{S/P})$. Thus, for all values of S/P ≤ 1, $f < f_0$. The variation of $q_{\max}$ with c_p in Fig. 8 shows that in this case $q_{\max}$ shows a weaker dependence on c_p than the theoretical value of

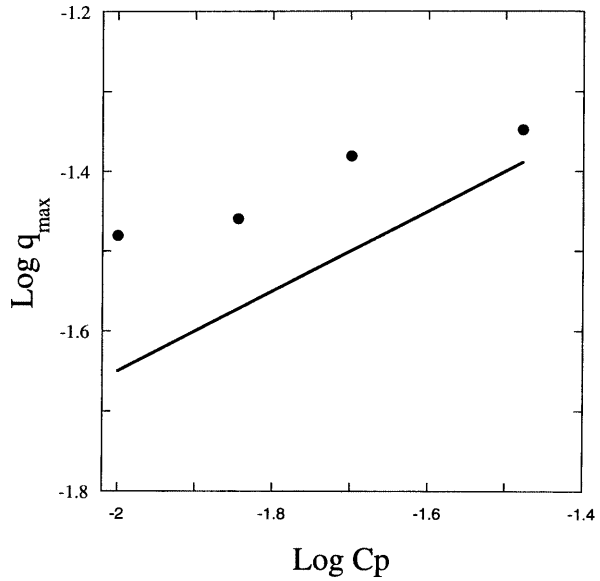

Fig. 8 Variation of peak position at intermediate q with polymer concentration deduced from polymer scattering curves. The *continuous line* has a slope of 0.5

0.5. This may be due to the irregular distribution of the charges on the copolymer; for PNIPAM homopolymer at similar concentrations, a $q_{\max} \sim c_{\mathrm{p}}^{0.5}$ dependence was observed [2].

Conclusion

We have investigated the solution behavior of a statistical copolymer containing hydrophilic and hydrophobic monomers. The observed behavior is neither that of a block copolymer (segregation of the insoluble sequences as would have been observed at temperature close to the LCST of the corresponding homopolymer) nor that of an alternating copolymer (no segregation at all). Instead, we have found an original behavior, where the copolymer undergoes a microphase separation at temperatures close to the LCST of the copolymer. This microphase separation allows the hydrophobic sequences of the macromolecules to segregate into water-free nodules, while the hydrophilic monomers remain in sequences bound to the surface of the nodules. In this situation, colloidal stability of the hydrophobic nodule is ensured by the steric repulsion of the hydrophilic sequences.

Addition of a small amount of an anionic surfactant does not change this behavior in a qualitative manner, although the colloidal particles are smaller. This can be attributed to the additional electrostatic repulsion of the particles due to adsorbed surfactants, which limits aggregation. In the presence of a large amount of surfactant, complete solubilization of the nodules is obtained. The insoluble sequences are now adsorbed on micellar aggregates forming a ‘‘necklace’’ structure.

Acknowledgements We thank G. Staikos for the generous gift of the copolymer and B. Demé and S. Egelhaaf for their assistance on the D11 and D22 spectrometers at ILL.

References

1. Schild HG, Tirrell DA (1991) Langmuir 7:665
2. Lee LT, Cabane B (1997) Macromolecules 30:6559
3. Kanda A, Duval M, Sarazin D, François J (1985) Polymer 6:406
4. Goddard ED (1993) In: Ananthapadmanabhan KP (ed) Interactions of surfactants with polymers and proteins. CRC Press, Boca Raton, pp 123
5. Mylonas Y, Karayanni K, Staikos G (1998) Langmuir 14:6320
6. Fisher ME, Burford RJ (1967) Phys Rev 156:583
7. Cabane B, Duplessix R (1982) J Phys (Paris) 43:1529
8. Cabane B, Duplessix R (1987) J Phys (Paris) 48:651
9. Nishida K, Kaji K, Kanaya T (1995) Macromolecules 28:2472
10. Essafi W (1996) Doctoral thesis. Université Paris VI
11. Pfeuty PJ (1978) Phys (Paris) Colloq 39:C2–149
12. Khokhlov AR, Khachaturian KA (1982) Polymer 23:1742
13. Kubota K, Fujishige S, Ando J (1990) Polym J 22:15